ELSEVIER

European Journal of Mechanics B/Fluids 21 (2002) 225–236

Interface stabilization in two-layer channel flow by surface heating or cooling

Ahmet Pinarbasi

Cukurova University, Mechanical Engineering Department, 01330 Balcali, Adana, Turkey

Received 13 August 2000; revised 9 May 2001 and 14 August 2001; accepted 14 September 2001

Abstract

The linear stability of plane Poiseuille flow of two immiscible Newtonian liquids in a differentially heated channel is considered. The equations of motion and energy are fully coupled via temperature-dependent fluid-viscosity coefficients. A long-wave asymptotic formulation of the stability problem is presented together with numerical results for disturbances of arbitrary wavelength. Two combinations of immiscible liquids are analyzed: silicone/water and oil/water (water at the bottom layer in both cases). It is shown that an imposed wall temperature difference can be stabilizing or destabilizing depending on the disturbance wavenumber and layer thickness ratio. Interfacial tension has a stabilizing effect on the interface. Stabilizing influence of interfacial tension is observed at intermediate and large wavenumbers. Most importantly, for certain ranges of the controlling dimensionless parameters, stable interfaces at all disturbance wavelengths can be attained.

Keywords: Channel flow; Interfacial stability; Spectral method; Heat transfer

1. Introduction

The problem of maintaining stable interfaces in two-fluid viscous flows is of considerable interest to many modern engineering flow processes. In the petroleum industry, for example, pumping costs in pipeline operations may be reduced considerably by adding a low viscosity fluid into the system. Experimental investigations of two-fluid pipe flow indicate that low viscosity fluids eventually encapsulate the more viscous fluids in both high and low Reynolds number flows [1,2]. A linear stability analysis of isothermal two-layer pipe flow shows that the flow is stable when the more viscous fluid occupies most of the pipe and that the volume ratio (or equivalently the layer thickness ratio) is a crucial factor in determining stable and unstable operating states. Renardy [3] studied the stability of two-layer Couette flow in configurations involving a thin layer near the wall and proved that while a thin layer of the more viscous liquid close to the wall is always linearly unstable, a thin layer of the less viscous liquid adjacent to the wall can be stable for all wavelengths provided there is adequate surface tension. These results have encouraged further research on the stability of two-fluid flow as applied to oil transportation and lubricated squeezing flows [4].

Interface stability is also of critical importance in coextrusion processes in the plastics industry where both planar and axisymmetric multi-layer flows are relevant. The coextrusion operation consists of combining several melt streams in a feedblock. The combined melt stream then flows to the die where the layers take their final dimensions. Under certain operating conditions, interfacial instabilities arise with detrimental effects on mechanical, optical, and barrier properties of the final product [5]. Efficient and robust control of the flow and suppression of instabilities is then of paramount importance in maintaining stable operating states.

E-mail address: ahpinar@mail.cu.edu.tr (A. Pinarbasi).

0997-7546/02/$ – see front matter
PII: S0997-7546(01)01169-4

Interfacial instabilities in two-layer viscous flows have been investigated by various authors under isothermal conditions. In his pioneering work, Yih [6] studied the stability of the interface using a long-wave asymptotic technique and showed that viscosity stratification alone can cause instability even at vanishingly small Reynolds numbers. Recent investigations examined the effect of disturbances of arbitrary wavelength on the stability of the interface for a wide range of viscosity, density, and thickness ratios [7–9].

In industrial coextrusion operations, fluid layers are frequently fed into the die at different temperatures in order to match viscosities and thus avoid interfacial instability. In general, considerable difficulties arise in adjusting material properties by varying temperatures [10]. Heat transfer and variable transport property effects on interfacial instability are poorly understood. Anturkar et al. [11] studied the interfacial instability of two-layer flow incorporating the temperature dependence of material properties but neglecting heat transfer across the layers and solving the standard isothermal stability equations. In a recent study, Pinarbasi and Liakopoulos [12] examined the stability of nonisothermal Poiseuille flow of two Newtonian liquids with temperature-dependent viscosity under the simplifying assumption of negligible temperature and viscosity fluctuations.

In the present study, the linear theory of interface stability for planar Poiseuille flow with heat transfer and variable viscosity, including temperature and viscosity fluctuations is formulated. The linearized equations describing the evolution of small, two-dimensional disturbances are derived for a differentially heated channel, and the stability problem is formulated as an eigenvalue problem for a set of four ordinary differential equations. The eigenvalue problem is solved asymptotically in the small wavenumber limit ($\alpha \to 0$) and numerically, by a pseudospectral method, for disturbances of arbitrary wavelength. The effects of the applied wall temperature difference and interfacial tension on the flow stability are discussed.

2. Governing equations

Consider the flow of two immiscible incompressible Newtonian liquids in a channel formed by two long parallel plates (Fig. 1). The flow is driven by a constant pressure gradient, and the channel walls are maintained at constant but different temperatures. Assuming that temperature variations predominantly affect the viscosity distribution and that thermal conductivity remains constant, the dimensionless governing equations (conservation of mass, momentum, and energy) take the form:

$$\nabla \cdot \mathbf{v}_k = 0, \tag{1}$$

$$\frac{\partial \mathbf{v}_k}{\partial t} + \mathbf{v}_k \cdot \nabla \mathbf{v}_k = -\frac{\nabla p_k}{r_k} + \frac{1}{r_k Re} \nabla \cdot (\mu_k \dot{\boldsymbol{\gamma}}_k), \tag{2}$$

$$\frac{\partial T_k}{\partial t} + \mathbf{v}_k \cdot \nabla T_k = \frac{m_k}{r_k Re Pr_k} \nabla^2 T_k, \tag{3}$$

where the dimensionless viscosity-temperature relation is assumed to be of the form

$$\mu_k = \frac{\bar{\mu}_k}{\bar{\mu}_{01}} = C_k m_k \exp\left(\frac{D_k}{T_k}\right). \tag{4}$$

The definitions of the non-dimensional variables are listed in Table 1. In Eqs. (1)–(4), subscript k denotes the layer number ($k = 1, 2$; no summation over k), $\dot{\boldsymbol{\gamma}}_k$ is the rate-of-strain tensor, $\mathbf{v}_k = (u_k, v_k)$ is the velocity vector, p_k denotes the pressure, T_k denotes the temperature, and $Pr_k = \bar{\mu}_{0k} \bar{c}_{pk} / \bar{k}_k$ denotes the Prandtl number for the kth layer. Here, $\bar{\mu}_0$, $\bar{c}_p$, and $\bar{k}$ denote the

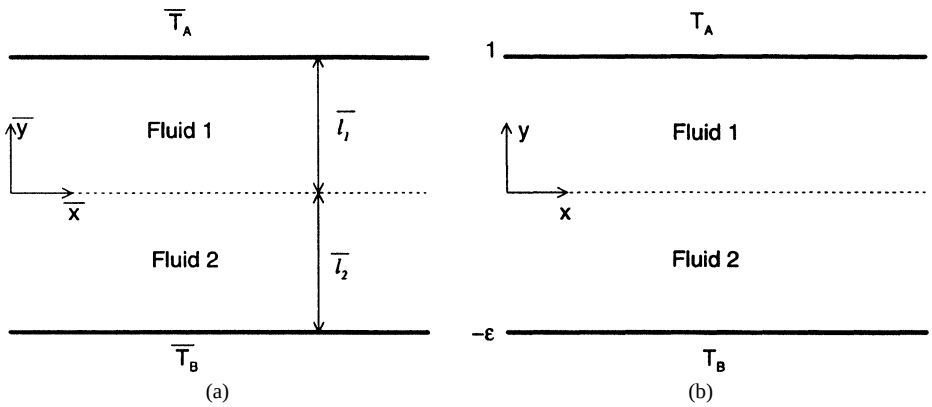

Fig. 1. Flow geometry and thermal boundary conditions: (a) dimensional; (b) dimensionless.

Table 1
Nondimensional variables. (Bars denote dimensional quantities.)

(x, y)	(u, v)	t	p	T_k	μ_k	m_k	r_k	D_k
$\frac{(\bar{x}, \bar{y})}{\bar{l}_1}$	$\frac{(\bar{u}, \bar{v})}{\overline{U}_0}$	$\frac{\bar{t}\overline{U}_0}{\bar{l}_1}$	$\frac{\bar{p}}{\bar{\rho}_1 \overline{U}_0^2}$	$\frac{\overline{T}_k}{\bar{d}_1}$	$\frac{\bar{\mu}_k}{\bar{\mu}_{01}}$	$\frac{\bar{\mu}_{0k}}{\bar{\mu}_{01}}$	$\frac{\bar{\rho}_k}{\bar{\rho}_1}$	$\frac{\bar{d}_k}{\bar{d}_1}$

viscosity, specific heat, and thermal conductivity of the fluids calculated at the reference temperature. Note that C_k, $k = 1, 2$, are dimensionless constants obtained from experimental temperature–viscosity curves and that (see Table 1) m_2 is the viscosity ratio at the reference temperature, r_2 is the density ratio, and D_2 is the viscosity-law exponent ratio. The Reynolds number is defined as $Re = \bar{\rho}_1 \overline{U}_0 \bar{l}_1 / \bar{\mu}_{01}$, where $\overline{U}_0$ is velocity at the interface and $\bar{l}_1$, $\bar{\rho}_1$, $\bar{\mu}_{01}$ denote the thickness, density, and viscosity (at the reference temperature) of layer 1 (top layer).

2.1. Basic state

In the undisturbed state, the flow is steady and fully developed. Considering a temperature profile that is independent of x and neglecting viscous dissipation, internal heat generation, and variable thermal conductivity effects, the energy balance equation yields a linear temperature profile within each layer. This solution of the energy equation is realizable only for isothermal channel walls. Note that the possibility of significant viscous dissipation exists in the coextrusion of viscous polymers. The goal here is to observe the influence of an imposed temperature gradient, and therefore, viscous dissipation is neglected for simplicity. Denoting the upper wall temperature by $\overline{T}_A$, the lower wall temperature by $\overline{T}_B$ and enforcing the continuity of temperature and heat flux at the interface, the dimensionless temperature distribution becomes

$$T_{s_k}(y) = D_k(S_k y + Q_k), \quad k = 1, 2, \tag{5}$$

where $S_k = \Delta\overline{T} A_k / \bar{d}_k$, $Q_k = (\varepsilon \Delta\overline{T} A_2 + \overline{T}_B)/\bar{d}_k$, $A_1 = K_2/(K_2 + \varepsilon)$, $A_2 = A_1/K_2$, $\varepsilon = \bar{l}_2/\bar{l}_1$ is the fluid-layer thickness ratio, $K_2 = \bar{k}_2/\bar{k}_1$ is the thermal conductivity ratio, $\Delta\overline{T} = \overline{T}_A - \overline{T}_B$ is the applied wall temperature difference, and the subscript s denotes conditions at the undisturbed state.

The x-component of the momentum equation takes the form

$$\left[\exp\left(\frac{1}{S_k y + Q_k}\right) u'_{s_k}\right]' = E_k, \quad k = 1, 2, \tag{6}$$

where u_{s_k} denotes the base velocity of the kth layer, $E_k = Re(\mathrm{d}p/\mathrm{d}x)/(C_k m_k)$, $\mathrm{d}p/\mathrm{d}x$ is the dimensionless pressure gradient, and primes denote differentiation with respect to y.

The associated boundary conditions (no-slip at the channel walls and continuity of velocity and shear stress at the interface) are

$$u_{s_1}(1) = u_{s_2}(-\varepsilon) = 0, \tag{7a}$$

$$u_{s_1}(0) = u_{s_2}(0), \tag{7b}$$

$$\mu_1(0) u'_{s_1}(0) = \mu_2(0) u'_{s_2}(0). \tag{7c}$$

The solution of Eq. (6) subject to Eq. 7(a–c) can be expressed in terms of exponential integrals:

$$\begin{aligned} u_{s_1}(y) \;=\; & \frac{E_1}{2S_1^2}\Bigg[(S_1 y + Q_1)(B_1 - Q_1 - 1 + S_1 y)\exp\left(-\frac{1}{S_1 y + Q_1}\right) \\ & - (S_1 + Q_1)(B_1 - Q_1 - 1 + S_1)\exp\left(-\frac{1}{S_1 + Q_1}\right) \\ & + (B_1 - 2Q_1 - 1)\left[E\left(\frac{1}{S_1 + Q_1}\right) - E\left(\frac{1}{S_1 y + Q_1}\right)\right]\Bigg], \end{aligned} \tag{8}$$

$$\begin{aligned} u_{s_2}(y) \;=\; & \frac{E_2}{2S_2^2}\Bigg[(S_2 y + Q_2)(B_2 - Q_2 - 1 + S_2 y)\exp\left(-\frac{1}{S_2 y + Q_2}\right) \\ & - (Q_2 - \varepsilon S_2)(B_2 - Q_2 - 1 - \varepsilon S_2)\exp\left(-\frac{1}{Q_2 - \varepsilon S_2}\right) \\ & + (B_2 - 2Q_2 - 1)\left[E\left(\frac{1}{Q_2 - \varepsilon S_2}\right) - E\left(\frac{1}{S_2 y + Q_2}\right)\right]\Bigg], \end{aligned} \tag{9}$$

where $E(x) = \int_x^\infty (\mathrm{e}^{-t}/t)\,\mathrm{d}t$ denotes the exponential integral,

$$B_1 = \frac{(C_2/C_1)m_2 f_3 + (S_1/S_2) f_4}{(C_2/C_1)m_2 f_2 - f_1}, \qquad B_2 = \frac{S_2}{S_1} B_1,$$

and

$$\begin{aligned}
f_1 &= \frac{Q_2}{S_2}\mathrm{e}^{-\frac{1}{Q_2}} - \frac{Q_2 - \varepsilon S_2}{S_2}\mathrm{e}^{-\frac{1}{Q_2-\varepsilon S_2}} + \frac{1}{S_2}\left[E\left(\frac{1}{Q_2-\varepsilon S_2}\right) - E\left(\frac{1}{Q_2}\right)\right],\\
f_2 &= \frac{Q_1}{S_1}\mathrm{e}^{-\frac{1}{Q_1}} - \frac{Q_1 + S_1}{S_1}\mathrm{e}^{-\frac{1}{Q_1+S_1}} + \frac{1}{S_1}\left[E\left(\frac{1}{Q_1+S_1}\right) - E\left(\frac{1}{Q_1}\right)\right],\\
f_3 &= \frac{Q_1 + Q_1^2}{S_1}\mathrm{e}^{-\frac{1}{Q_1}} + \frac{(Q_1+S_1)(S_1 - Q_1 - 1)}{S_1}\mathrm{e}^{-\frac{1}{Q_1+S_1}} + \frac{2Q_1+1}{S_1}\left[E\left(\frac{1}{Q_1+S_1}\right) - E\left(\frac{1}{Q_1}\right)\right],\\
f_4 &= -\frac{Q_2 + Q_2^2}{S_2}\mathrm{e}^{-\frac{1}{Q_2}} + \frac{(Q_2-\varepsilon S_2)(\varepsilon S_2 + Q_2 + 1)}{S_2}\mathrm{e}^{-\frac{1}{Q_2-\varepsilon S_2}} - \frac{2Q_2+1}{S_2}\left[E\left(\frac{1}{Q_2-\varepsilon S_2}\right) - E\left(\frac{1}{Q_2}\right)\right].
\end{aligned}$$

Note that the pressure gradient $\mathrm{d}p/\mathrm{d}x$ is determined by enforcing the condition $u_{s_1}(0) = 1$. Constants C_k and $\bar{d}_k$, $k = 1, 2$, depend on the liquids considered and reference temperature chosen.

2.2. Linear stability analysis

In this section, the stability problem is formulated by the method of normal modes [13]. Due to the complexity of the problem, the analysis is restricted to two-dimensional disturbances although there is no Squire's theorem for two-layer Poiseuille flow [7]. The velocity, pressure, temperature and viscosity fields are decomposed into two parts, the base fields and infinitesimal disturbances:

$$\begin{aligned}
u_k(x,y,t) &= u_{s_k}(y) + \hat{u}_k(x,y,t), \qquad v_k(x,y,t) = \hat{v}_k(x,y,t),\\
p_k(x,y,t) &= p_{s_k}(x) + \hat{p}_k(x,y,t). \qquad T_k(x,y,t) = T_{s_k}(y) + \widehat{T}_k(x,y,t),\\
\mu_k(x,y,t) &= \mu_{s_k}(y) + \hat{\mu}_k(x,y,t).
\end{aligned} \tag{10}$$

Substitution of Eq. (10) into Eqs. (1)–(3), subtraction of the base flow equations, and linearization lead to the disturbance evolution equations:

$$\frac{\partial \hat{u}_k}{\partial x} + \frac{\partial \hat{v}_k}{\partial y} = 0, \tag{11}$$

$$\begin{aligned}
\frac{\partial \hat{u}_k}{\partial t} + u_{s_k}\frac{\partial \hat{u}_k}{\partial x} + \hat{v}_k\frac{\mathrm{d}u_{s_k}}{\mathrm{d}y} &= -\frac{1}{r_k}\frac{\partial \hat{p}_k}{\partial x} + \frac{\mu_{s_k}}{Re\,r_k}\left(\frac{\partial^2 \hat{u}_k}{\partial x^2} + \frac{\partial^2 \hat{u}_k}{\partial y^2}\right) + \frac{\mu'_{s_k}}{Re\,r_k}\left(\frac{\partial \hat{u}_k}{\partial y} + \frac{\partial \hat{v}_k}{\partial x}\right) + \frac{u'_{s_k}}{Re\,r_k}\frac{\partial \hat{\mu}_k}{\partial y}\\
&\quad + \frac{\hat{\mu}_k}{Re\,r_k}\frac{\mathrm{d}^2 u_{s_k}}{\mathrm{d}y^2},
\end{aligned} \tag{12a}$$

$$\frac{\partial \hat{v}_k}{\partial t} + u_{s_k}\frac{\partial \hat{v}_k}{\partial x} = -\frac{1}{r_k}\frac{\partial \hat{p}_k}{\partial y} + \frac{\mu_{s_k}}{Re\,r_k}\left(\frac{\partial^2 \hat{v}_k}{\partial y^2} + \frac{\partial^2 \hat{v}_k}{\partial x^2}\right) + \frac{2\mu'_{s_k}}{Re\,r_k}\frac{\partial \hat{v}_k}{\partial y} + \frac{u'_{s_k}}{Re\,r_k}\frac{\partial \hat{\mu}_k}{\partial x}, \tag{12b}$$

$$\frac{\partial \widehat{T}_k}{\partial t} + u_{s_k}\frac{\partial \widehat{T}_k}{\partial x} + \hat{v}_k\frac{\mathrm{d}T_{s_k}}{\mathrm{d}y} = \frac{1}{Re\,r_k\,Pr_k}\left(\frac{\partial^2 \widehat{T}_k}{\partial x^2} + \frac{\partial^2 \widehat{T}_k}{\partial y^2}\right), \tag{13}$$

where primes denote differentiation with respect to y and $k = 1, 2$.

The continuity equation can be satisfied by introducing a perturbation streamfunction, $\hat{\psi}_k$, for each layer, i.e.,

$$\hat{u}_k = \frac{\partial \hat{\psi}_k}{\partial y}, \qquad \hat{v}_k = -\frac{\partial \hat{\psi}_k}{\partial x}, \quad k = 1, 2.$$

Since the coefficients of the perturbation equations are independent of x and t, it is assumed that all disturbances have time and spatial dependence of the form

$$\left(\hat{\psi}_k, \hat{p}_k, \widehat{T}_k, \hat{\mu}_k\right) = \left[\phi_k(y), f_k(y), \theta_k(y), \Lambda_k(y)\right]\mathrm{e}^{i\alpha(x-ct)}, \quad k = 1, 2, \tag{14}$$

where α is the wavenumber; $c = c_r + ic_i$ is the complex disturbance velocity; and ϕ_k, f_k, θ_k, and Λ_k denote the spatially varying velocity, pressure, temperature, and viscosity disturbance amplitudes, respectively. Note that instability is associated with $c_i > 0$.

Substituting Eq. (14) into Eqs. (12)–(13) and eliminating the pressure perturbation terms by cross-differentiation, the following stability equations are obtained:

$$i\alpha Re r_k\{(u_{s_k}-c)(\phi_k''-\alpha^2\phi_k)-u_{s_k}''\phi_k\} = \mu_{s_k}(\phi_k''''-2\alpha^2\phi_k''+\alpha^4\phi_k)+2\mu_{s_k}'(\phi_k'''-\alpha^2\phi_k')+\mu_{s_k}''(\phi_k''+\alpha^2\phi_k) + u_{s_k}'(\Lambda_k''+\alpha^2\Lambda_k)+2u_{s_k}''\Lambda_k'+u_{s_k}'''\Lambda_k, \quad k=1,2, \tag{15}$$

and

$$(i\alpha r_k Re Pr_k/m_k)\big[(u_{s_k}-c)\theta_k-T_{s_k}'\phi_k\big]=\theta_k''-\alpha^2\theta_k, \quad k=1,2. \tag{16}$$

Note that the amplitudes of viscosity and temperature perturbations are not independent. Specifically,

$$\Lambda_k(y)=\beta_k(y)\theta_k(y), \tag{17}$$

where

$$\beta_k(y)=-\frac{C_k m_k D_k}{T_{s_k}^2}\mathrm{e}^{D_k/T_{s_k}}. \tag{18}$$

Relation (17) is obtained by perturbing the viscosity law, expanding into Taylor series, and neglecting nonlinear terms.

The stability equations are subject to the following boundary conditions:

- no slip at the channel walls:

$$\phi_1=\phi_1'=0 \quad \text{at } y=1,$$
$$\phi_2=\phi_2'=0 \quad \text{at } y=-\varepsilon; \tag{19a}$$

- continuity of velocity at the interface:

$$\phi_1=\phi_2; \qquad \phi_1'-\phi_2'=\frac{\phi_1}{c-u_{s_1}}\{u_{s_2}'-u_{s_1}'\} \quad \text{at } y=0; \tag{19b}$$

- continuity of shear stress at the interface:

$$\mu_{s_1}(\phi_1''+\alpha^2\phi_1)+u_{s_1}'\beta_1\theta_1=\mu_{s_2}(\phi_2''+\alpha^2\phi_2)+u_{s_2}'\beta_2\theta_2 \quad \text{at } y=0; \tag{19c}$$

- continuity of normal stress at the interface:

$$\begin{aligned}&\mu_{s_2}\phi_2'''+\mu_{s_2}'\phi_2''-(3\mu_{s_2}\alpha^2+i\alpha Re r_2 u_{s_2})\phi_2'+(\mu_{s_2}'\alpha^2+i\alpha Re r_2 u_{s_2}')\phi_2-\mu_{s_1}\phi_1'''-\mu_{s_1}'\phi_1''\\ &\quad+(3\mu_{s_1}\alpha^2+i\alpha Re u_{s_1})\phi_1'-(\mu_{s_1}'\alpha^2+i\alpha Re u_{s_1}')\phi_1-c\big[i\alpha Re\phi_1'-i\alpha Re r_2\phi_2'\big]\\ &=i\alpha Re\big(F+\alpha^2 S\big)\frac{\phi_1}{c-u_{s_1}} \quad \text{at } y=0;\end{aligned} \tag{19d}$$

- constant temperature at the channel walls:

$$\theta_1=0 \quad \text{at } y=1, \qquad \theta_2=0 \quad \text{at } y=-\varepsilon; \tag{19e}$$

- continuity of temperature at the interface:

$$\frac{\phi_1}{c-u_{s_1}}\{T_{s_1}'-T_{s_2}'\}=\theta_2-\theta_1 \quad \text{at } y=0; \tag{19f}$$

- continuity of heat flux at the interface:

$$\theta_1'=K_2\theta_2' \quad \text{at } y=0. \tag{19g}$$

In the equations above, $S=\bar{\sigma}/(\bar{\rho}_1\overline{U}_0^2\bar{l}_1)$ and $F=(r_2-1)\bar{g}\bar{l}_1/\overline{U}_0^2$ are dimensionless groups accounting for the effects of interfacial tension and gravitational acceleration. It should be noted that the true interfacial conditions must be imposed at the deflected interface [6]. The linearized interfacial conditions (19b), (19c), (19d), (19f), (19g) were derived by considering Taylor series expansions about the undisturbed interface ($y=0$) and neglecting quadratic terms.

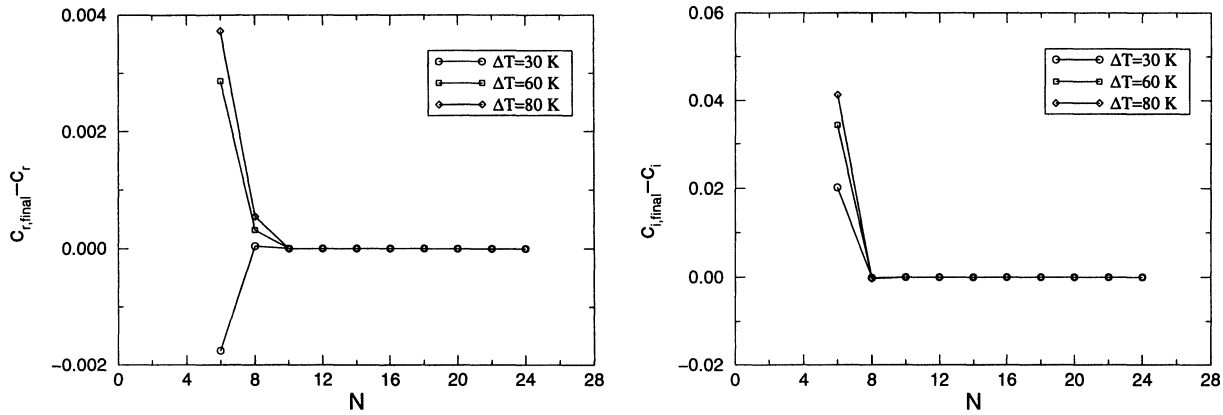

Fig. 2. Convergence test: (a) real, and (b) imaginary part of the complex disturbance velocity. $m_2 = 0.1$, $K_2 = 4.5$, $Pr_1 = 144$, $Pr_2 = 7.35$, $D_2 = 0.83$, $r_2 = 1$, $\varepsilon = 1$, $Re = 0.1$, $F = S = 0$, $\alpha = 1$.

2.3. Numerical solution

The linear stability problem formulated in the previous section is solved using a Chebyshev-pseudospectral technique. Each layer ($-\varepsilon \leqslant y \leqslant 0$ and $0 \leqslant y \leqslant 1$) is separately transformed into $-1 \leqslant Y \leqslant 1$, and in the transformed domain, the disturbance amplitudes ϕ_k, θ_k are expanded into series of Chebyshev polynomials of the first kind:

$$\phi_k = \sum_{n=0}^{N} a_n^{(k)} T_n(Y), \qquad \theta_k = \sum_{n=0}^{N} b_n^{(k)} T_n(Y), \quad k = 1, 2,$$

introducing a total of $4(N+1)$ unknowns.

The stability governing equations (Eqs. (15) and (16)) are enforced at the collocation points

$$Y_j = \cos\left(\frac{\pi j}{N-3}\right), \quad j = 0, 1, \ldots, N-3,$$

yielding $4(N-2)$ equations. These equations are augmented by the discrete versions of the 12 boundary conditions, bringing the total number of equations to $4(N+1)$. The formulation leads to a generalized matrix eigenvalue problem of the form $Ax = cBx$, which is solved using the IMSL routine *dgvccg*.

The convergence of the pseudospectral technique is tested in terms of the error in the eigenvalue with the smallest imaginary part. In Fig. 2, the errors in the real and imaginary parts of the eigenvalues are plotted versus the number of polynomials in the Chebyshev expansions for various wall temperature differences $\Delta\overline{T}$. The flow parameters are $m_2 = 0.1$, $K_2 = 4.5$, $Pr_1 = 144$, $Pr_2 = 7.35$, $D_2 = 0.83$, $r_2 = 1$, $\varepsilon = 1$, $Re = 0.1$, $F = S = 0$, and $\alpha = 1$. For each value of $\Delta\overline{T}$, the real and imaginary parts of the eigenvalue converge for values of N as small as ten. Typically, for small Re, up to $N = 16$ terms were used in each layer. For large values of the Reynolds number, N needs to be increased up to 30. The effect of collocation points on convergence of the eigenvalue problem is investigated in detail in [14].

3. Long-wave disturbances

In the long-wave asymptotic limit ($\alpha \to 0$), a regular expansion in powers of α is considered,

$$\begin{aligned}
&\phi_k \sim \phi_{0k} + \alpha\phi_{1k} + \mathrm{O}(\alpha^2), \quad k = 1, 2,\\
&\theta_k \sim \theta_{0k} + \alpha\theta_{1k} + \mathrm{O}(\alpha^2), \quad k = 1, 2,\\
&c \sim c_0 + \alpha c_1 + \mathrm{O}(\alpha^2).
\end{aligned} \tag{20}$$

Here, the first subscript denotes the order of approximation and the second subscript the layer number. Substituting into Eqs. (15), (16), (19a)–(19g) and comparing coefficients of α^n, we obtain a sequence of problems.

At α^0:

$$\mu_{s_k}\phi_{0k}'''' + 2\mu_{s_k}'\phi_{0k}''' + \mu_{s_k}''\phi_{0k}'' + u_{s_k}'\beta_k\theta_{0k}'' + \left(2u_{s_k}'\beta_k' + 2u_{s_k}''\beta_k\right)\theta_{0k}' + \left(u_{s_k}'\beta_k'' + 2u_{s_k}''\beta_k' + u_{s_k}'''\beta_k\right)\theta_{0k} = 0, \quad k = 1, 2, \tag{21a}$$

$$\theta_{0k}'' = 0, \quad k = 1, 2, \tag{21b}$$

subject to

$$\phi_{01} = \phi_{01}' = 0 \quad \text{at } y = 1, \qquad \phi_{02} = \phi_{02}' = 0 \quad \text{at } y = -\varepsilon, \tag{21c}$$

$$\phi_{01} = \phi_{02}; \qquad \phi_{01}' - \phi_{02}' = \frac{\phi_{01}}{c_0 - u_{s_1}}\left\{u_{s_2}' - u_{s_1}'\right\} \quad \text{at } y = 0, \tag{21d}$$

$$\mu_{s_1}\phi_{01}'' + u_{s_1}'\beta_1\theta_{01} = \mu_{s_2}\phi_{02}'' + u_{s_2}'\beta_2\theta_{02} \quad \text{at } y = 0, \tag{21e}$$

$$\mu_{s_2}\phi_{02}''' + \mu_{s_2}'\phi_{02}'' = \mu_{s_1}\phi_{01}''' + \mu_{s_1}'\phi_{01}'' \quad \text{at } y = 0, \tag{21f}$$

$$\theta_{01} = 0 \quad \text{at } y = 1, \qquad \theta_{02} = 0 \quad \text{at } y = -\varepsilon, \tag{21g}$$

$$\frac{\phi_{01}}{c_0 - u_{s_1}}\left\{T_{s_1}' - T_{s_2}'\right\} = \theta_{02} - \theta_{01} \quad \text{at } y = 0, \tag{21h}$$

$$\theta_{01}' = K_2\theta_{02}' \quad \text{at } y = 0. \tag{21i}$$

At α^1:

$$\mu_{s_k}\phi_{1k}'''' + 2\mu_{s_k}'\phi_{1k}''' + \mu_{s_k}''\phi_{1k}'' + (c_0 - u_{s_k})r_k i\,Re\,\phi_{0k}'' + u_{s_k}''r_k i\,Re\,\phi_{0k} + u_{s_k}'\beta_k\theta_{1k}'' + \left(2u_{s_k}'\beta_k' + 2u_{s_k}''\beta_k\right)\theta_{1k}' + \left(u_{s_k}'\beta_k'' + 2u_{s_k}''\beta_k' + u_{s_k}'''\beta_k\right)\theta_{1k} = 0, \quad k = 1, 2, \tag{22a}$$

$$\theta_{1k}'' + (c_0 - u_{s_k})(ir_k\,Re\,Pr_k/m_k)\theta_{0k} + \left(ir_k\,Re\,Pr_k\,T_{s_k}'/m_k\right)\phi_{0k} = 0, \quad k = 1, 2, \tag{22b}$$

subject to

$$\phi_{11} = \phi_{11}' = 0 \quad \text{at } y = 1, \qquad \phi_{12} = \phi_{12}' = 0 \quad \text{at } y = -\varepsilon, \tag{22c}$$

$$\phi_{11} = \phi_{12} \quad \text{at } y = 0, \tag{22d}$$

$$c_1\left(\phi_{01}' - \phi_{02}'\right) + (c_0 - u_{s_1})\left(\phi_{11}' - \phi_{12}'\right) = \phi_{11}\left\{u_{s_2}' - u_{s_1}'\right\} \quad \text{at } y = 0, \tag{22e}$$

$$\mu_{s_1}\phi_{11}'' + u_{s_1}'\beta_1\theta_{11} = \mu_{s_2}\phi_{12}'' + u_{s_2}'\beta_2\theta_{12} \quad \text{at } y = 0, \tag{22f}$$

$$\mu_{s_2}\phi_{12}''' + \mu_{s_2}'\phi_{12}'' + (c_0 - u_{s_2})r_2 i\,Re\,\phi_{02}' + u_{s_2}'r_2 i\,Re\,\phi_{02} - \mu_{s_1}\phi_{11}''' - \mu_{s_1}'\phi_{11}'' - (c_0 - u_{s_1})i\,Re\,\phi_{01}' - u_{s_1}'i\,Re\,\phi_{01} = \frac{i\,Re\,F\phi_{01}}{c_0 - u_{s_1}} \quad \text{at } y = 0, \tag{22g}$$

$$\theta_{11} = 0 \quad \text{at } y = 1, \qquad \theta_{12} = 0 \quad \text{at } y = -\varepsilon, \tag{22h}$$

$$\phi_{11}\left\{T_{s_1}' - T_{s_2}'\right\} + c_1(\theta_{01} - \theta_{02}) = (c_0 - u_{s_1})(\theta_{12} - \theta_{11}) \quad \text{at } y = 0, \tag{22i}$$

$$\theta_{11}' = K_2\theta_{12}' \quad \text{at } y = 0. \tag{22j}$$

Note that, in the limit $\alpha \to 0$, gravity ($F \neq 0$) does not enter the zeroth-order problem and interfacial tension ($S \neq 0$) enters neither the zeroth-nor the first-order problem. Furthermore, the zeroth-order solution is real and the first-order solution is purely imaginary. Therefore, stable/unstable conditions are determined by the sign of c_1.

Problems (21a–i) and (22a–j) along with the normalization equation

$$\phi_{01} + \alpha\phi_{11} = 1, \tag{22k}$$

were discretized by a Chebyshev-pseudospectral technique and the resulting system of equations was solved using the software package *minpack*.

To assess the accuracy of the stability calculations, the eigenvalues calculated by the method outlined in Section 2.3 is compared to those computed using the asymptotic formulation for $\alpha \to 0$ presented in this section. Table 2 shows that, for small α, the agreement is excellent.

Table 2
Comparison of asymptotic and numerical results. $m_2 = 0.1$, $K_2 = 4.5$, $Pr_1 = 144$, $Pr_2 = 7.35$, $D_2 = 0.83$, $r_2 = 1$, $\varepsilon = 1$, $Re = 0.1$, $F = S = 0$, $\alpha = 1 \times 10^{-3}$ and $N = 16$

$\Delta\overline{T}$ (K)	c (asymptotic)	c (numerical)
20	$1.55256 + i2.06709 \times 10^{-5}$	$1.55256 + i2.06703 \times 10^{-5}$
40	$1.43523 + i2.11223 \times 10^{-5}$	$1.43523 + i2.11230 \times 10^{-5}$
60	$1.32724 + i1.65480 \times 10^{-5}$	$1.32724 + i1.65477 \times 10^{-5}$
80	$1.23057 + i9.80570 \times 10^{-6}$	$1.23057 + i9.80524 \times 10^{-6}$

4. Results and discussion

Two combinations of immiscible liquids are considered: silicone/water and transformer oil/water (water at the bottom layer in both cases). Constants C_k and $\bar{d}_k$, $k = 1, 2$, are found from empirical viscosity–temperature curves for reference temperature $\overline{T}_{\text{ref}} = \overline{T}_{\text{cold}} = 20\ ^\circ\text{C}$ and are listed together with other relevant physical properties in Table 3. Dimensionless ratios that depend only on fluid transport properties are summarized in Table 4. Since the densities of silicone, transformer oil, and water are very close to each other at the reference temperature, the value of $r_2 = \bar{\rho}_2/\bar{\rho}_1$ is set equal to one. Note that $\overline{T}_{\text{cold}}$ is chosen as the reference temperature here and top (or bottom) wall is heated to create a temperature difference. Alternatively, $\overline{T}_{\text{hot}}$ could be chosen as reference temperature as well. In other words, heating or cooling of the fluid are terms that depend on the arbitrary choice of hot or cold wall temperatures as reference temperature. However, the stability governing equations would remain the same whether $\overline{T}_{\text{cold}}$ or $\overline{T}_{\text{hot}}$ is chosen as reference temperature. In order to prove this point, a test was performed by choosing $\overline{T}_{\text{ref}} = \overline{T}_{\text{hot}} = 100\ ^\circ\text{C}$ as reference temperature and the results are compared with $\overline{T}_{\text{ref}} = \overline{T}_{\text{cold}} = 20\ ^\circ\text{C}$ case. When $\overline{T}_{\text{hot}}$ is chosen as reference temperature, fluid properties take the following values for silicone/water pair: $C_1 = 3.722 \times 10^{-3}$, $\bar{d}_1 = 2087.2$ K, $C_2 = 9.601 \times 10^{-3}$, $\bar{d}_2 = 1733.6$ K, $Pr_1 = 39.11$, $Pr_2 = 1.75$, $m_2 = 0.13$, $D_2 = 0.83$, $K_2 = 5.85$. Results of this comparison is shown in Table 5. As one can see, the results are very close to each other, suggesting that results with respect to stabilization/destabilization are the same when reference temperature is changed from $\overline{T}_{\text{cold}}$ to $\overline{T}_{\text{hot}}$ You and Herwig [15] propose to use the centerline temperature $\overline{T}_c$ as reference temperature.

Table 3
Properties of fluids considered in this study

Liquid	$\bar{c}_p$ (20 °C) (kJ/kg·K)	$\bar{k}$ (20 °C) (W/m·K)	$\bar{\mu}$ (20 °C) (N·s/m^2)	$\bar{\mu}$ (100 °C) (N·s/m^2)	C	$\bar{d}$ (K)
Water	4.1818	0.598	1.0×10^{-3}	0.282×10^{-3}	2.702×10^{-3}	1733.6
Silicone	2.06	0.133	9.71×10^{-3}	2.11×10^{-3}	8.087×10^{-4}	2087.2
Transformer oil	4.2159	0.111	21.1×10^{-3}	1.741×10^{-3}	8.836×10^{-6}	3411.3

Table 4
Dimensionless ratios for silicone/water and transformer oil/water

$\frac{\text{Layer 1}}{\text{Layer 2}}$	m_2	K_2	Pr_1	Pr_2	D_2
$\frac{\text{Silicone}}{\text{Water}}$	0.1	4.5	144	7.35	0.83
$\frac{\text{Transformer oil}}{\text{Water}}$	0.05	6	325	7.35	0.53

Table 5
Reference temperature test for silicone/water pair. Fixed parameters: $Re = 0.1$, $F = S = 0$, $r_2 = 1$, $\varepsilon = 2$, $\Delta\overline{T} = 80$ K

α	c ($\overline{T}_B = \overline{T}_{\text{ref}} = 20\ ^\circ\text{C}$, heating from top)	c ($\overline{T}_A = \overline{T}_{\text{ref}} = 100\ ^\circ\text{C}$, cooling from bottom)
0.1	$1.5324 + i0.1305E{-}02$	$1.5342 + i0.1391E{-}02$
0.5	$1.3943 + i0.2481E{-}02$	$1.3902 + i0.2512E{-}02$
1.0	$1.2084 + i0.2397E{-}02$	$1.2022 + i0.2446E{-}02$
1.5	$1.1058 + i0.4279E{-}02$	$1.1025 + i0.4303E{-}02$
2.0	$1.0567 + i0.5103E{-}02$	$1.0535 + i0.5111E{-}02$

4.1. General remarks

The effect of temperature and viscosity fluctuations on the *shear* mode of instability in high-Reynolds-number *single layer* plane Poiseuille flow has been shown to be small [16,17]. In contrast, their effect on the *interfacial* mode of instability in *two-layer* flow can be significant, as can be seen in Fig. 3, where the disturbance growth rate is plotted against the disturbance wavenumber α for $\Delta\overline{T} = 10$ K and $\Delta\overline{T} = 50$ K. The flow system is silicone/water (see Table 4 for dimensionless parameters that depend on fluid transport properties) and the remaining parameters are set to $\varepsilon = 0.5$, $Re = 0.1$, $F = S = 0$. Curves corresponding to the simplified formulation, in which temperature and viscosity fluctuations are neglected, as well as curves corresponding to the full formulation, which includes all fluctuations, are presented for each $\Delta\overline{T}$. The effect of temperature and viscosity fluctuations is appreciable for wavenumbers $\alpha \lesssim 8$, and, as expected, becomes more pronounced as the applied wall temperature difference $\Delta\overline{T}$ increases. All results presented in the remaining part of this paper are obtained based on the full formulation.

Typical profiles of the disturbance streamfunction amplitude, ϕ, and disturbance temperature amplitude, θ, are shown in Figs. 4 and 5. In both figures, a transformer oil/water combination is considered (see Table 4) and $\varepsilon = 1$, $F = S = 0$, $\alpha = 3$. Each eigenvector of the generalized matrix eigenanalysis problem $A\boldsymbol{x} = cB\boldsymbol{x}$ is normalized by setting its Euclidean norm equal to unity. In Fig. 4, $\Delta\overline{T}$ is varied while in Fig. 5, the effect of the Reynolds number is shown. The streamfunction amplitude reaches its maximum in the vicinity of the interface while the maximum temperature amplitude is located at the interface. As expected on physical grounds, increasing the wall temperature difference $\Delta\overline{T}$ affects predominantly the temperature amplitude distribution, while *Re* affects mostly the disturbance streamfunction amplitude and to a lesser degree the disturbance temperature amplitude.

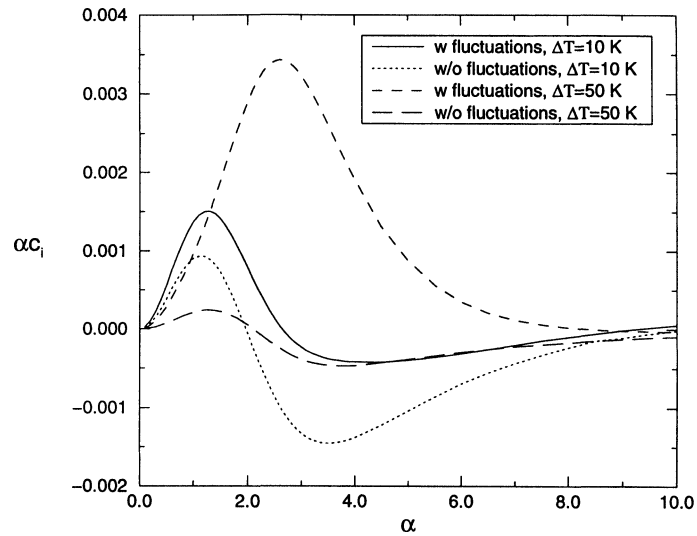

Fig. 3. Effect of temperature and viscosity fluctuations on the growth rate of disturbances. Silicone/water, $r_2 = 1$, $\varepsilon = 0.5$, $Re = 0.1$, $F = S = 0$.

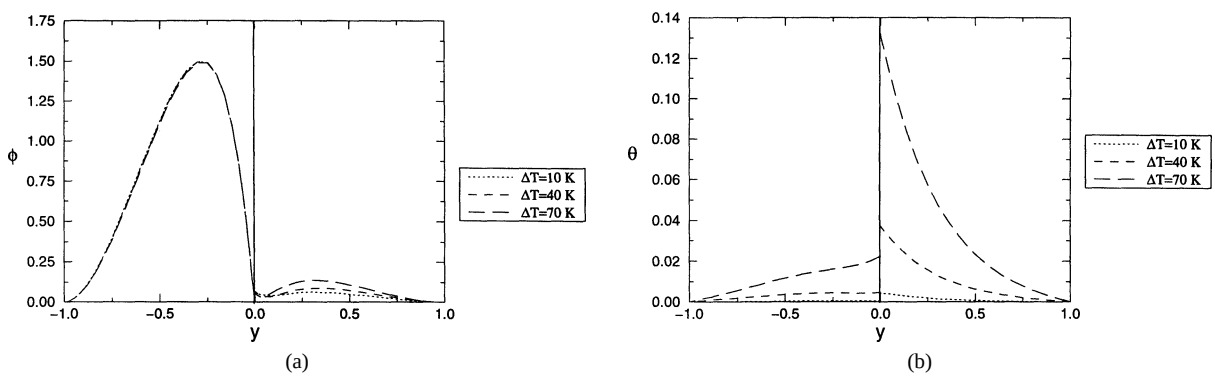

Fig. 4. Amplitude of disturbance streamfunction (a), and disturbance temperature (b) for various $\Delta\overline{T}$. Transformer oil/water, $r_2 = 1$, $\varepsilon = 1$, $Re = 0.1$, $F = S = 0$, and $\alpha = 3$.

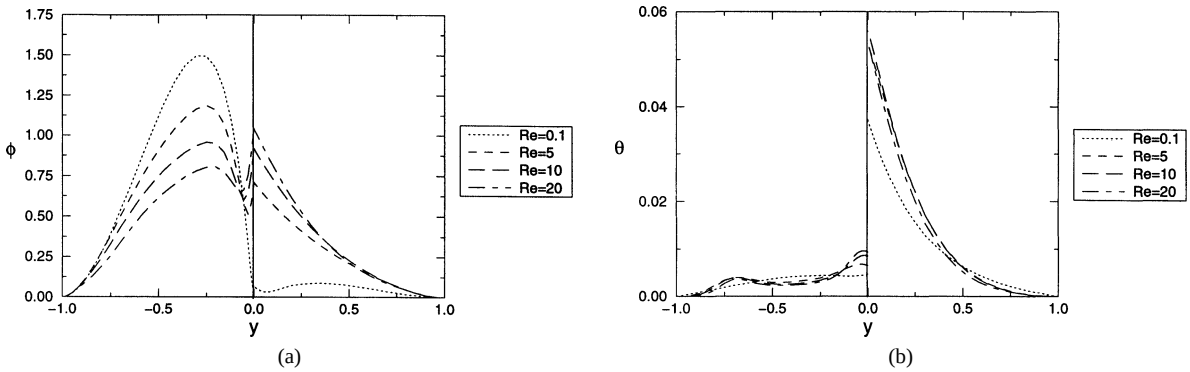

Fig. 5. Amplitude of disturbance streamfunction (a), and disturbance temperature (b) for various Reynolds numbers. Transformer oil/water, $r_2 = 1$, $\varepsilon = 1$, $F = S = 0$, $\alpha = 3$, $\Delta\overline{T} = 40$ K.

4.2. Stabilizing the interface

The effect of $\Delta\overline{T}$ on the marginal stability curves in the $(\alpha$–$\varepsilon)$ plane is presented in Fig. 6. The liquid pair is silicone/water and (Re, F, S) is set to $(0.1, 0, 0)$. Positive $\Delta\overline{T}$ corresponds to a hot top wall, while negative values of $\Delta\overline{T}$ signify a hot bottom wall. Note that in the present study, $\overline{T}(y) \geqslant \overline{T}_{\text{ref}} = \overline{T}_{\text{cold}} = 20\ ^\circ\text{C}$. Consequently, since the viscosity of both liquids decreases as $|\Delta\overline{T}|$ increases, the maximum of the dimensionless base velocity shifts towards the upper wall when the top wall is heated, while the maximum of the dimensionless base velocity shifts towards the lower wall when the bottom wall is heated. Under isothermal conditions and in the absence of surface tension, the flow configuration with $\varepsilon = \sqrt{m_2} =$ constant is neutrally stable to disturbances of all wavenumbers (see Fig. 6(a)). For this configuration, the slope of the base velocity is zero at the interface, and hence continuous across the interface. Under nonisothermal conditions, the neutral stability line $\varepsilon = \sqrt{m_2}$ disappears. The structure of the marginal stability curves depend strongly on the sign of $\Delta\overline{T}$. When the upper plate is heated, the unstable regions in the $(\alpha$–$\varepsilon)$ plane grow at the expense of stable regions as $\Delta\overline{T}$ increases (see Fig. 6(a–c)). When the lower plate is heated, increasing $|\Delta\overline{T}|$ can be stabilizing or destabilizing depending on the values of ε and α (see Fig. 6(d–e)). A thin layer of the less viscous fluid adjacent to the wall (small ε) becomes unstable to disturbances of long and intermediate wavelengths.

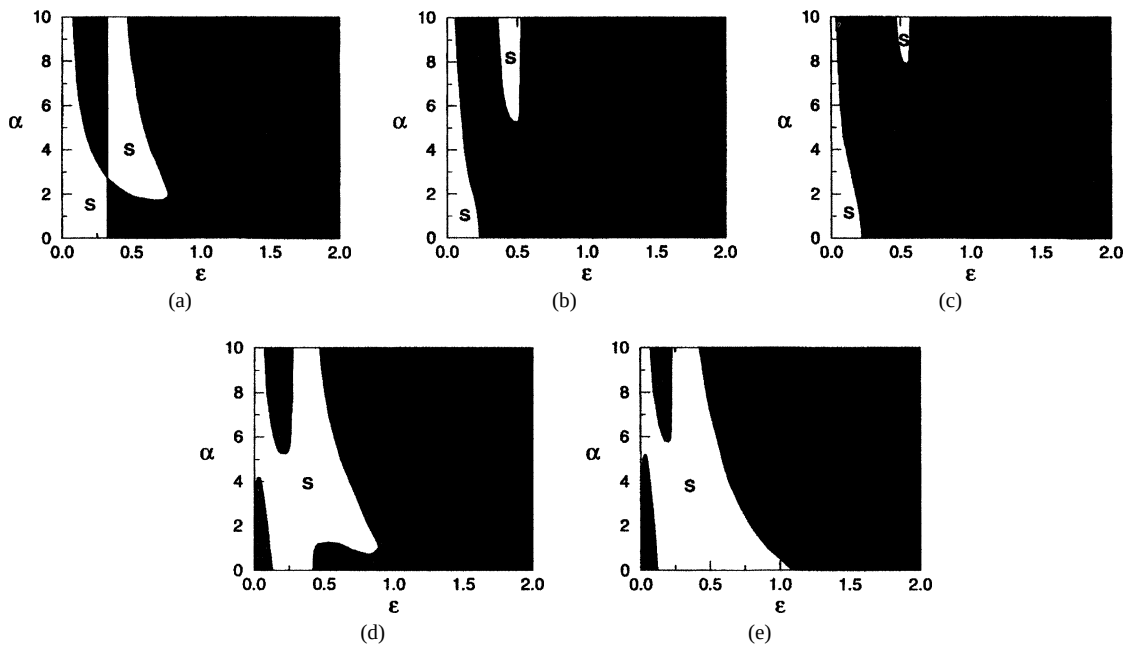

Fig. 6. Marginal stability curves for various wall temperature differences $\Delta\overline{T}$. Silicone/water, $r_2 = 1$, $Re = 0.1$, $F = S = 0$. Shaded regions are unstable, unshaded regions are stable: (a) $\Delta\overline{T} = 0$ K; (b) $\Delta\overline{T} = 20$ K; (c) $\Delta\overline{T} = 50$ K; (d) $\Delta\overline{T} = -20$ K; (e) $\Delta\overline{T} = -50$ K.

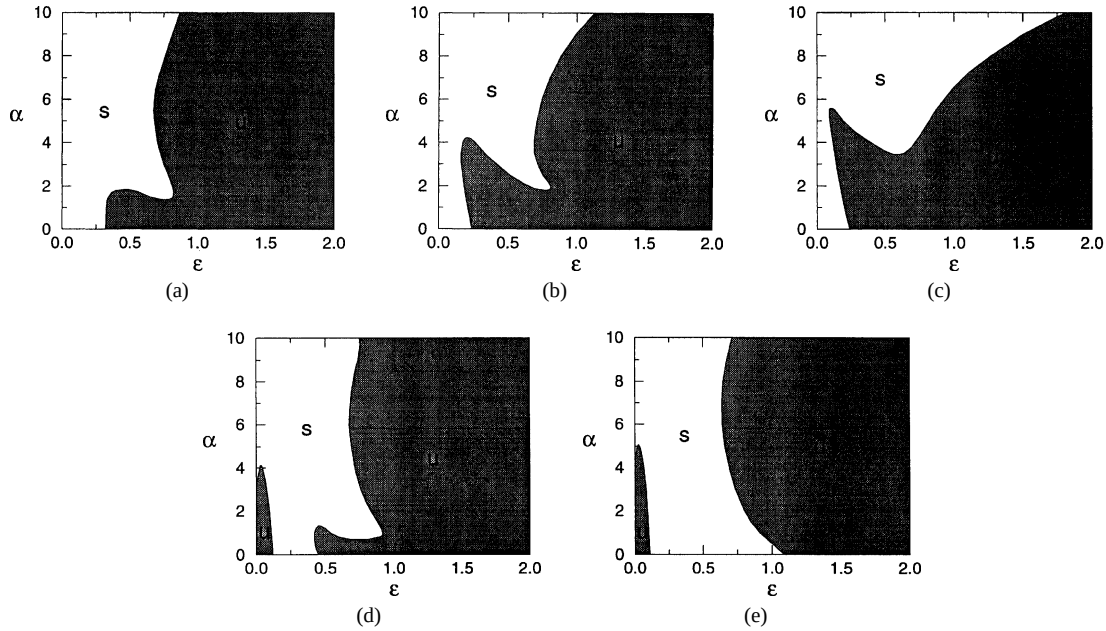

Fig. 7. Marginal stability curves for $S = 0.01$. Silicone/water, $r_2 = 1$, $Re = 0.1$, $F = 0$, $S = 0.01$: (a) $\Delta\overline{T} = 0$ K; (b) $\Delta\overline{T} = 20$ K; (c) $\Delta\overline{T} = 50$ K; (d) $\Delta\overline{T} = -20$ K; (e) $\Delta\overline{T} = -40$ K.

This unstable region in the (α–ε) plane grows towards higher values of α as $|\Delta\overline{T}|$ increases. On the other hand, maintaining the lower wall at a higher temperature stabilizes long-, intermediate- and short-wave disturbances for configurations around $\varepsilon \approx 0.3$. For $0.24 \lesssim \varepsilon \lesssim 0.43$ and $\Delta\overline{T} = -50$ K, the system is stable for all α. This means that, by heating the bottom plate, we can achieve a window of stable operating conditions in practical applications.

The combined effect of surface heating and interfacial tension is shown in Fig. 7. In all cases $S = 0.01$, which is a reasonable value for silicone/water system. The remaining parameter values are identical to those of Fig. 6. When $\Delta\overline{T} = 0$, comparison of Fig. 7(a) with Fig. 6(a) reveals that the inclusion of interfacial tension ruptures the neutral stability line $\varepsilon = \sqrt{m_2}$. In general, in the presence of interfacial tension, an applied positive or negative wall temperature difference can be stabilizing or destabilizing depending on the values of ε and α. Fig. 7(a–c) shows that the stable region observed for small values of ε decreases as $\Delta\overline{T}$ increases. More importantly, a comparison of Fig. 6(d–e) and Fig. 7(d–e) shows that, for $\Delta\overline{T} < 0$, interfacial tension stabilizes shortwaves ($\alpha > 5$), and increasing $|\Delta\overline{T}|$ predominantly stabilizes disturbances of $\alpha < 2$. As a result of the combined effects of nonzero S and increasing $|\Delta\overline{T}|$, the width of the stable operating window of Fig. 6 is increased to $0.11 \lesssim \varepsilon \lesssim 0.63$ (compare Figs. 6(e) and 7(e)).

Note that in high-Reynolds-number single-layer plane Poiseuille flow, an imposed wall temperature difference $\Delta\overline{T}$ is always destabilizing (see [18] for water flow; also [16]). In contrast, for the interfacial instability mode in the two-layer flow considered here, increasing the magnitude of the applied wall temperature difference can be stabilizing or destabilizing depending on the disturbance wavenumber, the flow configuration (thickness ratio), and the sign of $\Delta\overline{T}$.

In isothermal flow, a thin layer of the more viscous fluid adjacent to the wall is always linearly unstable, while a thin layer of the less viscous fluid adjacent to the wall is stable provided that there is enough surface tension at the interface (see, for example, [19,2,3]). This phenomenon is usually referred to as the ‘thin layer’ effect. For the flow systems chosen in this study, the more viscous liquid lies at the upper layer and consequently $\varepsilon \gg 1$ corresponds to a thin layer of the more viscous liquid adjacent to the upper wall. Examining Figs. 6 and 7, it is seen that the results, even under nonisothermal conditions, are in agreement with the thin layer effect reported for isothermal flows. Note that although the analysis is extended for ε up to 10, here marginal stability curves are presented only for $0 \leqslant \varepsilon \leqslant 2$ or sometimes $0 \leqslant \varepsilon \leqslant 3$. The flow is always unstable for large values of ε. Figures 6(b–c) and 7(b–c) show that stable configurations of thin layers of the less viscous fluid next to the wall ($\varepsilon \ll 1$ in the present study) persist in the case of positive wall temperature difference $\Delta\overline{T}$. Configurations with $\varepsilon \ll 1$ are stable to disturbances of wavenumber $0 < \alpha < 10$ although this region contracts slightly as $\Delta\overline{T}$ increases. On the other hand, when $\Delta\overline{T} < 0$, thin layers of the less viscous fluid next to the wall are stable only for intermediate to short wavelengths (see Figs. 6(d–e) and 7(d–e)). For long and lower-intermediate wavelengths, there is an unstable region which propagates to intermediate wavelengths as $|\Delta\overline{T}|$ increases. This result contrasts the stability results reported for isothermal plane Poiseuille flow [6] and for isothermal Couette flow [19] where a thin layer of the less viscous fluid is stable to long-wave disturbances.

5. Conclusions

A linear stability analysis of nonisothermal two-layer plane Poiseuille flow has been presented. The temperature profile is assumed linear within each layer and the viscosity-temperature relation is exponential. Two-dimensional velocity, pressure, temperature, and viscosity fluctuations are included in the analysis. The role of varying the applied temperature difference $\Delta\overline{T}$ and interfacial tension S is investigated.

The stability of the interface is primarily investigated for two combinations of immiscible liquids: silicone/water and oil/water (water at the bottom layer in both cases). The analysis indicates that in the absence of density stratification, increasing the wall temperature difference $\Delta\overline{T}$ can stabilize or destabilize the interface depending on the layer thickness ratio and the disturbance wavelength. Interfacial tension has a stabilizing effect on the interface. The stabilizing influence of surface tension is observed at intermediate and large wavenumbers. A thin layer of the more viscous liquid adjacent to the wall ($\varepsilon \gg 1$ in this study) is found to be always unstable under isothermal as well as nonisothermal conditions. In contrast, a thin layer of the less viscous fluid next to the wall ($\varepsilon \ll 1$ in the present study) is stable for all wavelengths if the system is heated from the top and enough interfacial tension is present. If the lower wall is maintained at higher temperature, interfaces corresponding to $\varepsilon \ll 1$ are stable to disturbances of intermediate and large wavenumbers only. Most importantly, the results suggest that by heating the flow system from the bottom and having adequate surface tension, one can obtain large stable operating windows ($\varepsilon_0 - \Delta\varepsilon \lesssim \varepsilon \lesssim \varepsilon_0 + \Delta\varepsilon$) where the flow system is stable to disturbances of any wavelength.

Acknowledgments

The author would like to thank Professor Antonios Liakopoulos for his guidance and many invaluable suggestions throughout the conduct of this research.

References

[1] Yu H.S., Sparrow E.M., Experiments on two-component stratified flow in a horizontal duct, Trans. ASME C: J. Heat Transfer 91 (1969) 51–58.
[2] Joseph D.D., Renardy M., Renardy Y., Instability of the flow of two immiscible liquids with different viscosities in a pipe, J. Fluid Mech. 141 (1984) 309–317.
[3] Renardy Y., The thin-layer effect and interfacial stability in a two-layer Couette flow with similar liquids, Phys. Fluids 30 (1987) 1627–1637.
[4] Joseph D.D., Renardy Y.Y., Fundamentals of Two-fluid Dynamics, Springer-Verlag, 1993.
[5] Han C.D., Multiphase Flow in Polymer Processing, Academic Press, 1981.
[6] Yih C.S., Instability due to viscosity stratification, J. Fluid Mech. 27 (1967) 337–352.
[7] Yiantsios S.G., Higgins B.G., Linear stability of plane Poiseuille flow of two superposed fluids, Phys. Fluids 31 (1988) 3225–3238.
[8] Anturkar N.R., Papanastasiou T.C., Wilkes J.O., Linear stability analysis of multilayer plane Poiseuille flow, Phys. Fluids 2 (1990) 530–541.
[9] Pinarbasi A., Liakopoulos A., Stability of two-layer Poiseuille flow of Carreau–Yasuda and Bingham-like fluids, J. Non-Newtonian Fluid Mech. 57 (1995) 227–241.
[10] Nordberg M.E., Winter H.H., A simple model of nonisothermal coextrusion, Polym. Eng. Sci. 30 (1990) 408–415.
[11] Anturkar N.R., Wilkes J.O., Papanastasiou T.C., Estimation of critical stability parameters by asymptotic analysis in multilayer extrusion, Polym. Eng. Sci. 33 (1993) 1532–1539.
[12] Pinarbasi A., Liakopoulos A., The effect of variable viscosity on the interfacial stability of two-layer Poiseuille flow, Phys. Fluids 7 (1995) 1318–1324.
[13] Drazin P.G., Reid W.H., Hydrodynamic Stability, Cambridge University Press, 1981.
[14] Pinarbasi A., Formulation and computational issues for stability of two-layer inelastic fluids, Comput. Fluids 29 (2000) 1–16.
[15] You X., Herwig, H., Linear stability of channel flow with heat transfer: The important role of reference temperature, Int. Comm. Heat Mass Transfer 24 (1997) 485–496.
[16] Pinarbasi A., Liakopoulos A., The role of variable viscosity in the stability of channel flow, Int. Comm. Heat Mass Transfer 22 (1995) 837–847.
[17] Schäfer P., Herwig H., Stability of plane Poiseuille flow with temperature dependent viscosity, Int. J. Heat Mass Transfer 36 (1993) 2441–2448.
[18] Potter M.C., Graber E.J., Stability of plane Poiseuille flow with heat transfer, NASA TN D-6027, 1970.
[19] Hooper A.P., Long-wave instability at the interface between two viscous fluids: Thin layer effects, Phys. Fluids 28 (1985) 1613–1618.